

Alma Mater Studiorum Università di Bologna  
Archivio istituzionale della ricerca

Decoupled d-q Axes Current-Sharing Control of Multi-Three-Phase Induction Machines

This is the final peer-reviewed author's accepted manuscript (postprint) of the following publication:

*Published Version:*

Sala, G., Mengoni, M., Rizzoli, G., Zarri, L., Tani, A. (2020). Decoupled d-q Axes Current-Sharing Control of Multi-Three-Phase Induction Machines. IEEE TRANSACTIONS ON INDUSTRIAL ELECTRONICS, 67, 7124-7134 [10.1109/TIE.2019.2941127].

*Availability:*

This version is available at: <https://hdl.handle.net/11585/706988> since: 2024-02-27

*Published:*

DOI: <http://doi.org/10.1109/TIE.2019.2941127>

*Terms of use:*

Some rights reserved. The terms and conditions for the reuse of this version of the manuscript are specified in the publishing policy. For all terms of use and more information see the publisher's website.

This item was downloaded from IRIS Università di Bologna (<https://cris.unibo.it/>).  
When citing, please refer to the published version.

(Article begins on next page)

# Decoupled d-q Axes Current Sharing Control of Multi Three-Phase Induction Machines

Giacomo Sala, Michele Mengoni, Gabriele Rizzoli, Luca Zarri, *Senior Member, IEEE*, and Angelo Tani

**Abstract**—Multi three-phase drives are a particular case of multiphase systems, which are often used in high-power applications, such as wind-energy generation, naval and railway propulsion. In a multi three-phase system the electric machine is fed by more than one three-phase converter. A current sharing algorithm for multi three-phase drives allows setting unequal current references among the converters so that each of them differently contributes to the generation of the magnetic torque and flux. Suitable current sharing control systems already exist and have been presented for multi three-phase machines. This paper illustrates a current sharing technique where the contributions to the rotor flux for the three-phase inverters, related to the d-axis current, is decoupled from the contributions to the electromagnetic torque, which depends on the q-axis current. Also, the presented algorithm minimizes the Joule losses in the stator winding.

Finally, the advantages of the proposed method are analyzed and confirmed by experimental tests. The effectiveness of the control strategy is validated on a scaled prototype of a quadruple three-phase starter/generator for more-electric-aircraft applications.

**Index Terms**—Induction motors, machine vector control, multiphase drives, power sharing, variable speed drives.

## NOMENCLATURE

|                |   |
|----------------|---|
| $j$            | Imaginary unit ( $j^2 = -1$ ).  |
| $*$            | Complex conjugate operator.   |
| $i, v, \phi$   | Main electrical quantities: current ( $i$ ), voltage ( $v$ ) and flux linkage ( $\phi$ ).   |
| $m$            | Number of phases.   |
| $N_{star}$     | Number of star-connected three-phase subsystems.  |
| $x_{TV,V,W}$   | Quantity $x$ of the phase $U$ , $V$ or $W$ related to the $T$ th three-phase winding.   |
| $\varphi_T$    | Angular position of the magnetic axis of phase $U$ of the $T$ th three-phase winding in the stator reference frame (in electrical radians). |
| $\bar{y}_\rho$ | Space vector in the complex plane (space) $\alpha_\rho - \beta_\rho$ of the quantity $y$ .  |

|              |  |
|--------------|--|
| $S, R$       | Superscripts $S$ and $R$ are used to identify space vectors represented in the stator or rotor reference frames. Subscripts $S$ and $R$ are used to distinguish between stator and rotor quantities. |
| $\theta$     | Rotor flux angle (in electrical radians).  |
| $d, q$       | Subscripts used for the representation of space vector components along the direct and quadrature axes of the rotor flux reference frame.  |
| $R_S$        | Stator phase resistance.   |
| $R_{R,\rho}$ | Equivalent rotor resistance in the $\rho$ th subspace.   |
| $P_J$        | Stator Joule losses.   |
| $K_{Td,q}$   | Direct ( $d$ ) or quadrature ( $q$ ) axis current sharing coefficients for the $T$ th three-phase winding.   |
| $\omega_m$   | Rotor angular speed (in electrical radians).   |
| $\omega$     | Rotor flux angular speed (in electrical radians).  |

## I. INTRODUCTION

WHEN the electrical machines are not directly connected to the grid, the number of phases can be arbitrary and becomes a potential design variable. This degree of freedom results in higher performance, reliability and control flexibility [1]. The advantages of a multiphase drive depend on the considered machine topology, but some of them are intrinsic. In particular, multiphase machines allow splitting the total power of the system among a higher number of phases. Reducing the power on each phase results in a derating of the power switches of the converter that feeds the machine. This advantage is essential for high power applications, such as wind generators [2], electric ship propulsion systems [3], high power turbo compressors [4] and More Electric Aircraft (MEA) systems [5], [6], but it is also suitable for low voltage drives, e.g., in high-speed elevators [7] and automotive industry [8].

Among the types of multiphase machines, the multi three-phase one, composed of several three-phase sub-windings, shows significant advantages over the three-phase counterpart. Firstly, it allows using a standard three-phase inverter technology, without requiring the redesign of the converter. Then, the PWM modulation technique of each three-phase subsystem can be managed as in a traditional three-phase drive by using the third harmonic injection technique to fully exploit the available dc-link voltage. Otherwise, more sophisticated techniques must be used to optimize the performance and voltage range of multiphase inverters [9], [10].

Also, multiphase drives present higher control flexibility. In a star-connected three-phase winding, it is possible to independently control only two currents because the sum of

Manuscript received January 31, 2019; revised May 12, 2019, and July 19, 2019; accepted August 29, 2019. Copyright (C) 2019 IEEE. Personal use of this material is permitted. However, permission to use this material for any other purposes must be obtained from the IEEE, by sending a request to pubs-permissions@ieee.org.

The authors are with the Department of Electrical, Electronic and Information Engineering "Guglielmo Marconi", University of Bologna, 40136 Bologna, Italy (e-mail: giacomo.sala5@unibo.it, michele.mengoni@unibo.it, gabriele.rizzoli@unibo.it, luca.zarri2@unibo.it, angelo.tani@unibo.it).

Coloured version of one or more of the figures in this article are available on-line at <http://ieeexplore.ieee.org>.

the three currents is equal to zero. Conversely, in an  $m$ -phase multiphase machine with a single star point, the number of independent currents is  $m - 1$ , whereas the independent currents are  $(m - N_{star})$  in case of  $N_{star}$  star points.

The higher number of independent currents corresponds to enhanced controllability of the harmonics of the magnetic field in the airgap. By means of the technique known as Vector Space Decomposition (VSD), it is possible to map each harmonic of the magnetic field in the air-gap onto a specific Vector Space (VS) or subspace of the machine model. The control of the voltage and current Space Vectors (SVs) in a different subspace allows managing more field harmonics, which can be employed to improve the drive performance by limiting the torque harmonics [11] or to control the radial force on the rotor [12], and to improve the torque capability [13]. Finally, another interesting feature of a multi three-phase drive is that the current of each three-phase inverter can be controlled to generate a level of power that is independent of the others, provided that the sum of all the output powers is equal to the one requested by the load. In particular, it is even possible to reverse the power flow of a converter with respect to the remaining ones, as shown in Fig. 1. The concept of independent setpoints for the currents, which goes under the name of current sharing control, is discussed in this paper. Many algorithms have already been proposed to control multi three-phase synchronous machines with unbalanced current flows [14]–[17]. The same concept has also been investigated for Induction Machines (IMs). Two inverters of a double three-phase machine connected in parallel to the same dc link are considered in [18], showing the possibility of controlling the drive with good dynamics even when an inverter shuts off. In [19], a dual three-phase machine is fed by two inverters having dc links connected in series. The power of the first winding of the dual three-phase machine is controlled in a different way from the second one in order to balance the voltage of the dc link capacitors of the inverters. Control techniques for power-sharing have also been proposed for IMs [20]–[23], a triple three-phase IM [20], and a quadruple three-phase configuration [21], [22]. In these manuscripts, the current sharing has been implemented by splitting the reference current vector of the machine in smaller vectors but aligned with the reference vector. In [23], the authors developed a power sharing technique for a double three-phase IM which indirectly decouples the d and q current components, aiming to redistribute the machine active and reactive powers among the two inverters.

The present work illustrates a general approach for current sharing algorithms based on the introduction of separate coefficients to decouple the d and q components of the current vector of each inverter from the fundamental current vector of the multi three-phase IM. This control technique introduces new scenarios, presented in Section IV, which are not feasible by means of the control strategies presented in [20]–[23]. The generalization of the control system for a machine with a generic number of windings and the definition of the setpoints for the minimum stator Joule losses are the main contributions of this paper.

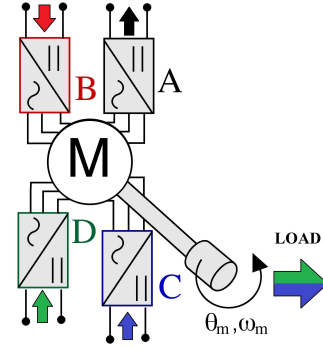


Fig. 1. Example of power flows in a quadruple three-phase drive in case of power sharing control. Inverter A is generating a power which is the opposite of the one fed by the inverter B. Neglecting the drive losses, the power transferred to the load is the sum of the power fed by C and D.

## II. MACHINE EQUATIONS

The model of a multi three-phase machine can be derived by considering each three-phase subsystem independently and then summing the effects of all the subsystems, under the assumption that the iron core has a negligible saturation. The use of SV transformations is a common approach to model three-phase machines and can be easily extended to multi three-phase typologies as described in the following subsections. In order to have a clear understanding of the proposed control algorithm, the model of the multi three-phase machine considers only the fundamental harmonic of the magnetic field in the air-gap, and the squirrel cage is represented by its simplified equivalent circuit. Despite these approximations, it is commonly assumed that the resulting model can be used for the analysis and the development of current sharing algorithms for induction machines [20].

### A. Space Vector Representation of Multi Three-Phase Windings

The electrical quantities of a symmetric three-phase machine, with phases U, V and W, can be represented by means of the following SV transformation:

$$\bar{y}_\rho = \frac{2}{3}(x_U + x_V e^{j\rho\frac{2\pi}{3}} + x_W e^{j\rho\frac{4\pi}{3}}), \quad \rho = 0, 1, \dots, \infty \quad (1)$$

where  $\bar{y}_\rho$  is the SV in the  $\rho_{th}$  complex plane (space)  $\alpha_\rho - \beta_\rho$ . Equation (1) for  $\rho = 1$  and  $\rho = 0$  leads to the following relationships:

$$\bar{y}_1 = \frac{2}{3}(x_U + x_V e^{j\frac{2\pi}{3}} + x_W e^{j\frac{4\pi}{3}}) \quad (2)$$

and

$$y_0 = \frac{2}{3}(x_U + x_V + x_W) \quad (3)$$

where the complex number  $\bar{y}_1$  is the SV in the complex plane (space)  $\alpha_1 - \beta_1$ , while  $y_0$  is referred to as the zero sequence component (or common mode component). The SVs of a three-phase machine with  $\rho > 1$  can be related to  $\bar{y}_1$  and  $y_0$  as follows:

$$\begin{aligned} \bar{y}_\rho &= \bar{y}_1 & \text{if } \rho &= 3n + 1 \\ \bar{y}_\rho &= \bar{y}_1^* & \text{if } \rho &= 3n - 1 \quad n = 1, 2, \dots, \infty. \\ \bar{y}_\rho &= y_0 & \text{if } \rho &= 3n \end{aligned} \quad (4)$$

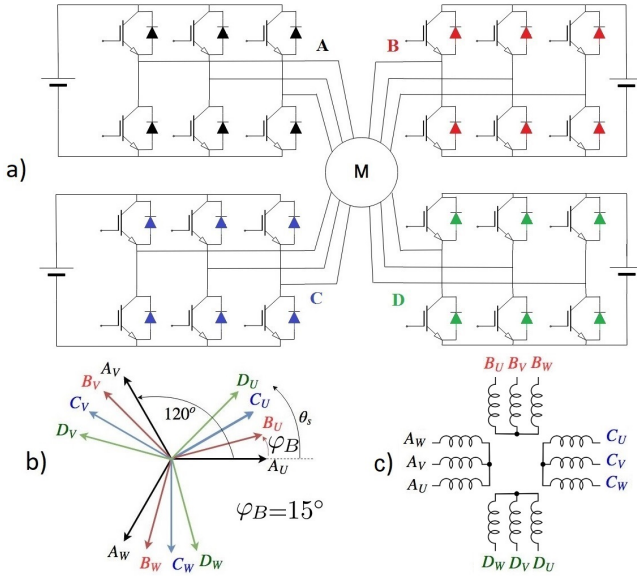


Fig. 2. Layout of a quadruple three-phase drive (a), distribution of the magnetic axes of the quadruple three-phase machine (b) and star connection layout (c). The phase shift between the three-phase subsystems is 15 electrical degrees.

Therefore, from (2) and (3), the inverse transform can be written as follows:

$$\begin{aligned} x_U &= \frac{y_0}{2} + \Re\{\bar{y}_1\} \\ x_V &= \frac{y_0}{2} + \Re\{\bar{y}_1 e^{-j\frac{2\pi}{3}}\} \\ x_W &= \frac{y_0}{2} + \Re\{\bar{y}_1 e^{-j\frac{4\pi}{3}}\}. \end{aligned} \quad (5)$$

The transformation (1) can be extended to a multi three-phase winding as follows:

$$\bar{y}_\rho = \frac{1}{N_{star}} \sum_{T=1}^{N_{star}} \frac{2}{3} (x_{TU} + x_{TV} e^{j\rho\frac{2\pi}{3}} + x_{TW} e^{j\rho\frac{4\pi}{3}}) e^{j\rho\varphi_T}, \quad \rho = 0, 1, \dots, \infty \quad (6)$$

where  $N_{star}$  is the number of three-phase windings (as example,  $N_{star} = 4$  in a layout as the one in Fig. 2(c)) and  $\varphi_T$  is the displacement angle in electrical radians of the magnetic axis of phase U of the  $T$ th three-phase winding from the axis of the stator reference frame. In case of symmetrically distributed winding, the displacement angle of the  $T$ th winding is

$$\varphi_T = \frac{2\pi}{3N_{star}} (T - 1) \quad (7)$$

while, in case of asymmetrical distributed winding, it is

$$\varphi_T = \frac{\pi}{3N_{star}} (T - 1). \quad (8)$$

As an example of asymmetrical winding, Fig. 2(b) shows the distribution of the magnetic axes of a quadruple three-phase machine, where the three-phase sub-windings have been named respectively with letters A, B, C and D. The general

inverse transformation can be defined for the  $T$ th winding as follows:

$$\begin{aligned} x_{TU} &= \frac{1}{2} \sum_{\rho=0}^{m-1} \Re\{\bar{y}_\rho e^{-j\rho\varphi_T}\} \\ x_{TV} &= \frac{1}{2} \sum_{\rho=0}^{m-1} \Re\{\bar{y}_\rho e^{-j\rho\frac{2\pi}{3}} e^{-j\rho\varphi_T}\} \\ x_{TW} &= \frac{1}{2} \sum_{\rho=0}^{m-1} \Re\{\bar{y}_\rho e^{-j\rho\frac{4\pi}{3}} e^{-j\rho\varphi_T}\} \end{aligned} \quad (9)$$

where  $m$  is the total number of phases ( $m = 3N_{star}$ ).

In case of a symmetrical winding with an odd number of phases ( $N_{star}$  is odd), the inverse transform (9) can be simplified as follows:

$$\begin{aligned} x_{TU} &= \frac{y_0}{2} + \sum_{\rho_{odd}=1}^{m-2} \Re\{\bar{y}_\rho e^{-j\rho\varphi_T}\} \\ x_{TV} &= \frac{y_0}{2} + \sum_{\rho_{odd}=1}^{m-2} \Re\{\bar{y}_\rho e^{-j\rho\frac{2\pi}{3}} e^{-j\rho\varphi_T}\} \\ x_{TW} &= \frac{y_0}{2} + \sum_{\rho_{odd}=1}^{m-2} \Re\{\bar{y}_\rho e^{-j\rho\frac{4\pi}{3}} e^{-j\rho\varphi_T}\}. \end{aligned} \quad (10)$$

Conversely, in case of an asymmetrical winding with an even number of phases ( $N_{star}$  is even), the inverse transform (9) can be simplified as shown in (11).

$$\begin{aligned} x_{TU} &= \sum_{\rho_{odd}=1}^{m-1} \Re\{\bar{y}_\rho e^{-j\rho\varphi_T}\} \\ x_{TV} &= \sum_{\rho_{odd}=1}^{m-1} \Re\{\bar{y}_\rho e^{-j\rho\frac{2\pi}{3}} e^{-j\rho\varphi_T}\} \\ x_{TW} &= \sum_{\rho_{odd}=1}^{m-1} \Re\{\bar{y}_\rho e^{-j\rho\frac{4\pi}{3}} e^{-j\rho\varphi_T}\}. \end{aligned} \quad (11)$$

Equations (6)-(11) can be used to model multi three-phase machines.

## B. Model of a Multi Three-Phase Induction Machine

By applying the SV transformation (6) to all the electrical quantities of a multi three-phase IM, the stator and rotor voltage equations can be written in terms of SVs in the respective reference frames as follows:

$$\bar{v}_{S,\rho}^S = R_S \bar{i}_{S,\rho}^S + \frac{d\bar{\phi}_{S,\rho}^S}{dt} \quad (12)$$

and

$$0 = R_{R,\rho} \bar{i}_{R,\rho}^R + \frac{d\bar{\phi}_{R,\rho}^R}{dt} \quad (13)$$

where  $\bar{i}$ ,  $\bar{v}$  and  $\bar{\phi}$  are the SVs of the currents, voltages and flux linkages,  $R_S$  is the stator phase resistance, and  $R_{R,\rho}$  is the equivalent rotor resistance in the  $\rho$ th subspace. It is assumed that the stator reference frame is the one of the first phase winding.

In a standard three-phase drive, it is common that the stator and rotor SVs are described in the reference frame aligned

with the rotor flux  $\bar{\phi}_{R,1}$ . For a multiphase machine, the same approach can be extended to each  $\rho$ th space. In these reference frames, the rotor flux  $\bar{\phi}_{R,\rho}$  can be controlled by adjusting the related d component of the stator current. Similarly, the torque contribution of each subspace can be controlled by the corresponding q component of the stator current. However, the main interaction between the stator and the rotor is caused by the fundamental harmonic of the magnetic field in the airgap, and the model can be simplified by neglecting the interaction of high-order harmonics (for  $\rho > 1$ ). This allows considering only the electrical equations in the fundamental subspace ( $\rho = 1$ ) to describe the electromagnetic behaviour of the machine. Therefore, the machine control becomes similar to that of a three-phase machine, because the SV  $\bar{i}_1$  of the stator currents is defined by (6) as follows:

$$\bar{i}_1^S = \frac{1}{N_{star}} \sum_T \bar{i}_{T1}^S e^{j\varphi_T} \quad (14)$$

where  $\bar{i}_{T1}^S$  is the three-phase SV of the  $T$ th inverter evaluated with (2). For simplicity, in (14) and from now on, the subscript "S" has been removed, assuming that all the variables are related to the stator quantities.

The higher order SVs can be defined manipulating (6) as:

$$\bar{i}_\rho^S = \frac{1}{N_{star}} \sum_T \bar{i}_{T\rho}^S e^{j\rho\varphi_T}. \quad (15)$$

Since the zero sequence current of each three-phase winding  $i_{T0}$  is zero due to the star connections, (4) can be rewritten for the current SVs of each  $T$ th winding, resulting in the following relationships:

$$\begin{aligned} \bar{i}_{T\rho}^S &= \bar{i}_{T1}^S & \text{if } \rho = 3n + 1 \\ \bar{i}_{T\rho}^S &= \bar{i}_{T1}^{S*} & \text{if } \rho = 3n - 1 \quad n = 1, 2, \dots, \infty \\ \bar{i}_{T\rho}^S &= 0 & \text{if } \rho = 3n. \end{aligned} \quad (16)$$

Equation (16) expresses all the SVs of the  $T$ th inverter as a function of  $\bar{i}_{T1}^S$ .

The current SV  $\bar{i}_1^S$  in (14) can be expressed in the rotor flux reference frame by applying the conventional Park transformation:

$$\bar{i}_1 = \bar{i}_1^S e^{-j\theta} = i_{1d} + j i_{1q} \quad (17)$$

where  $\theta$  is the electrical position of the rotor flux in the stator reference frame  $\alpha_1 - \beta_1$  (axis  $\alpha_1$  is aligned with the magnetic axis of phase  $U$  of the first three-phase winding).

By defining  $\bar{i}_{T1}$  for the  $T$ th winding as

$$\bar{i}_{T1} = \bar{i}_{T1}^S e^{j(\varphi_T - \theta)} \quad (18)$$

equation (6) can be rewritten in the rotor flux reference frame as

$$\bar{i}_1 = \frac{1}{N_{star}} \sum_T \bar{i}_{T1} = \frac{1}{N_{star}} \sum_T (i_{T1d} + j i_{T1q}) \quad (19)$$

to emphasize the d-q components of the stator currents. This equation will be used in Section III to analyze the problem of the current sharing.

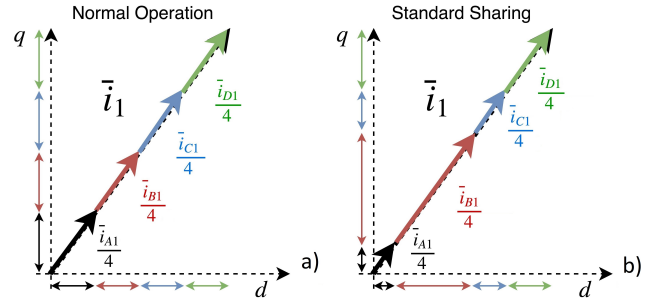


Fig. 3. Schematic explanation of the machine control in normal operation (a) and with a standard current sharing method (b) for a quadruple three-phase IM fed by inverters A, B, C and D.

### III. CURRENT SHARING

Equation (19) is the fundamental current sharing equation. According to the traditional Field Oriented Control (FOC) algorithm, the control algorithm of the machine consists in tracking the reference value of  $\bar{i}_1$ , which is the sum of the SVs  $\bar{i}_{T1}$  (with  $T = A, B, \dots$ ) for a multi three-phase machine with  $N_{star}$  windings.

To implement a current sharing algorithm, it is necessary to introduce  $N_{star}$  sharing coefficients:

$$\bar{K}_T = \frac{\bar{i}_{T1}}{N_{star} \bar{i}_1} \quad (T = A, B, \dots). \quad (20)$$

Combining (19) and (20) leads to the following constraint:

$$\sum_T \bar{K}_T = 1. \quad (21)$$

The standard current-sharing algorithm for multi three-phase IMs assumes that all coefficients  $\bar{K}_T$  are real numbers. This means that the contributions of the three-phase subsystems to  $\bar{i}_1$  are in phase with one another, as shown in Fig. 3(a). To minimize the total stator Joule losses all these coefficients must be equal. However, when the controlled current has to be unequally split among the converters, the standard current sharing algorithm (an example is shown in Fig. 3(b)) is not the best solution, and the method proposed in the next section provides better performance in terms of Joule stator losses.

### IV. OPTIMISED CURRENT SHARING: D-Q AXES DECOUPLING

The standard current sharing technique shares the d component of the stator current SV  $\bar{i}_1$  in the same way as the q-axis one. Also, it is well known that the q-axis current of each three-phase subsystem is related to torque production, whereas the d component contributes to the generation of the rotor flux. Therefore, it seems reasonable to improve the current sharing technique by decoupling the d-axis algorithm from the q-axis one. This can be done by introducing two sharing coefficients for each winding:

$$K_{Td} = \frac{i_{T1d}}{N_{star} i_{1d}}, \quad K_{Tq} = \frac{i_{T1q}}{N_{star} i_{1q}}. \quad (22)$$

Substituting (22) in (19), one obtains:

$$\bar{i}_1 = i_{1d} \sum_T K_{Td} + j i_{1q} \sum_T K_{Tq}. \quad (23)$$

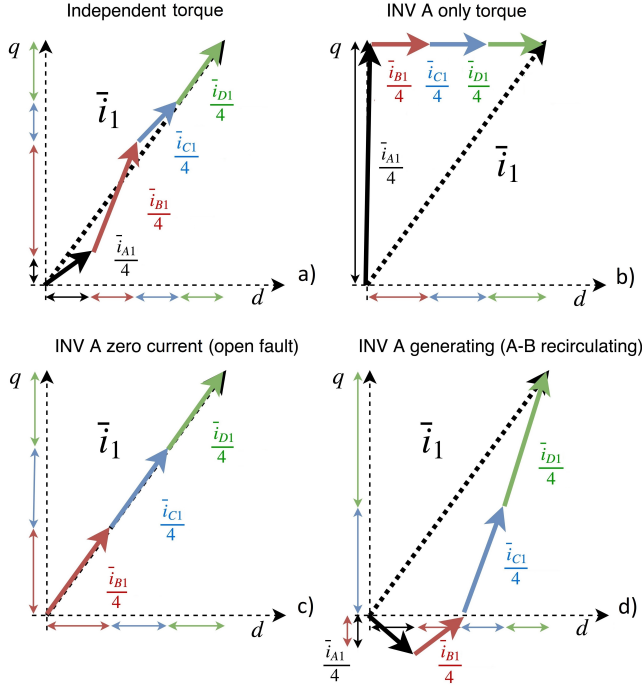


Fig. 4. Most significant decoupled current sharing examples for a quadruple three-phase layout (A,B,C,D): independent torque sharing with equally distributed rotor flux control (a); A is controlled to produce only torque (b); A is working at zero current (open fault) (c); A is generating opposite reference current and the others are supplying the power for the load and for the converter A (with recirculating power between A and B) (d).

Equation (23) leads to the following constraints for the sharing coefficients:

$$\sum_T K_{Td} = 1, \quad \sum_T K_{Tq} = 1. \quad (24)$$

Finally, the current SV of each three-phase subsystem can be found with (18), as follows:

$$\vec{i}_{T1}^S = \vec{i}_{T1} e^{j(\theta - \varphi_T)} = (K_{Td} i_{1d} + j K_{Tq} i_{1q}) N_{star} e^{j(\theta - \varphi_T)}. \quad (25)$$

Among the possible sharing control techniques, it is worth mentioning four particular cases:

- (a) all the subsystems equally contribute to the rotor flux of the machine but not to the electromagnetic torque. The coefficient  $K_{Td}$  is  $1/N_{star}$  for all converters;
- (b) the  $X$ th converter does not contribute to the electromagnetic torque or to the machine rotor flux:  $K_{Xd} = 0$  or  $K_{Xq} = 0$ ;
- (c) the current of the  $F$ th converter is set to zero:  $K_{Fd} = K_{Fq} = 0$ ;
- (d) the current of the  $Y$ th converter is reversed (recirculating power):  $K_{Yq} < 0$ , and  $K_{Tq} > 0$  for  $T \neq Y$ .

Fig. 4 shows the vector diagram of the SVs of the converter currents for a quadruple three-phase machine in these four cases. Case (a) is the most interesting under healthy operation of the drive and allows minimizing the stator Joule losses when the converters unequally contribute to the electromagnetic torque. Other optimization techniques could be taken into account, such as, for example, the drive efficiency or the

distribution of the losses managed by each inverter. However, to the best of the authors' knowledge, the minimization of the stator Joule losses is the simplest strategy that can be generalized to an arbitrary number of three-phase windings without any dependence on the system parameters. The stator Joule losses can be defined by combining (11), (15) and (16) as follows:

$$P_J = \sum_{k=1}^m R_s i_k^2 = \sum_{\rho_{odd}=1}^{m-1} \frac{m}{2} R_s |\vec{i}_\rho^S|^2 = \sum_T \frac{3}{2} R_s |\vec{i}_{T1}^S|^2. \quad (26)$$

By considering (25), (26) can be rewritten in the d-q reference frame as:

$$P_J = \frac{3}{2} N_{star}^2 R_s [i_{1d}^2 \sum_T K_{Td}^2 + i_{1q}^2 \sum_T K_{Tq}^2]. \quad (27)$$

It turns out that, given the constraints (24), the minimum of the stator Joule losses is obtained when the sum of the squares of both the d-axis and q-axis current sharing coefficients is at minimum. If there are not further constraints in the current contributions, this condition is met when the coefficients are equal to each others:

$$K_{Td} = K_d = \frac{1}{N_{star}}, \quad K_{Tq} = K_q = \frac{1}{N_{star}}. \quad (28)$$

Replacing (28) in (27) leads to the conventional equation for the stator Joule losses:

$$P_J = \frac{3}{2} N_{star} R_s (i_{1d}^2 + i_{1q}^2). \quad (29)$$

Conversely, when the inverters do not equally contribute to the generation of the electromagnetic torque (rotor flux control), the related q-axis (d-axis) sharing coefficients  $K_{Tq}$  ( $K_{Td}$ ) are different from each others, and the total stator Joule losses are expected to increase according to (27). In particular, if some sharing coefficients are predetermined for particular purposes, the solution that minimizes the stator Joule losses is the one that minimizes the sum of the squares of the remaining sharing coefficients (the ones not fixed by the control requirements). Since the sum of the sharing coefficients is constrained by (24), the minimum of the sum of their square values is reached when the available sharing coefficients are equal. Therefore, the optimization of the current-sharing algorithm is not based on a numerical approach, but it comes from the analysis of the equations of the model. Finally, it is important to note that case (c) has been mentioned because it represents a particular current sharing algorithm that can also be used as a possible post-fault control strategy if the switches of an inverter are turned off (this is the most common post-fault strategy in commercial three-phase inverters) [18], [24], [25].

## V. CURRENT SHARING CONTROL OF A QUADRUPLE THREE-PHASE INDUCTION MACHINE

Hereafter, the analysis focuses on a quadruple three-phase machine to illustrate the concepts presented in Sections II-IV and the control system for a multi three-phase drive under current sharing operation.

In particular, for the quadruple three-phase machine of Fig. 2, the displacement angle between the corresponding magnetic

axes of two neighbouring three-phase subsystems is 15 electrical degrees. The angular position  $\varphi_T$  of the magnetic axis of the first phase of the  $T$ th winding can be expressed with the relationship  $\varphi_T = \frac{\pi}{12}(t(T) - 1)$ , where  $t(T)$  is a function defined as follows:

$$t(T) = \begin{cases} 1 & \text{if } T = A \\ 2 & \text{if } T = B \\ 3 & \text{if } T = C \\ 4 & \text{if } T = D \end{cases} \quad (30)$$

and the SVs involved in the inverse transformation (11) are the 1<sup>st</sup> (the main SV), 3<sup>rd</sup>, 5<sup>th</sup>, 7<sup>th</sup>, 9<sup>th</sup> and 11<sup>th</sup> (auxiliary SVs), defined by (15). Furthermore, owing to the star connection of each winding, (16) imposes that the 3<sup>rd</sup> and 9<sup>th</sup> current SVs are zero.

### A. Optimised Current Sharing Equations

It results from (15) and (16) that the current SVs of the subspaces 5, 7 and 11 ( $\bar{i}_5^S$ ,  $\bar{i}_7^S$ ,  $\bar{i}_{11}^S$ ) can be written as:

$$\begin{aligned} \bar{i}_5^S &= \frac{1}{4} \sum_{T=A,B,C,D} \bar{i}_{T5}^S e^{j5\varphi_T} = \frac{1}{4} \sum_{T=A,B,C,D} \bar{i}_{T1}^{S*} e^{j5\frac{\pi}{12}(t(T)-1)} \\ \bar{i}_7^S &= \frac{1}{4} \sum_{T=A,B,C,D} \bar{i}_{T7}^S e^{j7\varphi_T} = \frac{1}{4} \sum_{T=A,B,C,D} \bar{i}_{T1}^S e^{j7\frac{\pi}{12}(t(T)-1)} \\ \bar{i}_{11}^S &= \frac{1}{4} \sum_{T=A,B,C,D} \bar{i}_{T11}^S e^{j11\varphi_T} = \frac{1}{4} \sum_{T=A,B,C,D} \bar{i}_{T1}^{S*} e^{j11\frac{\pi}{12}(t(T)-1)} \end{aligned} \quad (31)$$

Once  $i_{1d}$ ,  $i_{1q}$ ,  $K_{Td}$  and  $K_{Tq}$  ( $T = A, B, C, D$ ) are known, the reference multiphase current SVs in (31) are respectively defined in the stationary reference frame by (25) as:

$$\begin{aligned} \bar{i}_5^S &= \sum_{T=A,B,C,D} [K_{Td}i_{1d} - jK_{Tq}i_{1q}] e^{j(5+1)\frac{\pi}{12}(t(T)-1)} e^{-j\theta} \\ \bar{i}_7^S &= \sum_{T=A,B,C,D} [K_{Td}i_{1d} + jK_{Tq}i_{1q}] e^{j(-7+1)\frac{\pi}{12}(t(T)-1)} e^{j\theta} \\ \bar{i}_{11}^S &= \sum_{T=A,B,C,D} [K_{Td}i_{1d} - jK_{Tq}i_{1q}] e^{j(11+1)\frac{\pi}{12}(t(T)-1)} e^{-j\theta} \end{aligned} \quad (32)$$

To simplify (32), a reference frame synchronous with the main component of the rotor flux ( $\bar{\phi}_{R,1}$ ) should be used to represent the current vector mapped in subspace 7, and a counter-rotating reference frame for the subspaces 5 and 11. The resulting transformations are:

$$\begin{aligned} \bar{i}_5^S &= \bar{i}_{5-} e^{-j\theta} \\ \bar{i}_7^S &= \bar{i}_{7+} e^{j\theta} \\ \bar{i}_{11}^S &= \bar{i}_{11-} e^{-j\theta} \end{aligned} \quad (33)$$

Therefore, combining (32) and (33), the expressions of  $\bar{i}_{5-}$ ,  $\bar{i}_{7+}$  and  $\bar{i}_{11-}$  become:

$$\begin{aligned} \bar{i}_{5-} &= (K_{Ad} + jK_{Bd} - K_{Cd} - jK_{Dd})i_{1d} + \\ &\quad - j(K_{Aq} + jK_{Bq} - K_{Cq} - jK_{Dq})i_{1q} \\ \bar{i}_{7+} &= (K_{Ad} - jK_{Bd} - K_{Cd} + jK_{Dd})i_{1d} + \\ &\quad + j(K_{Aq} - jK_{Bq} - K_{Cq} + jK_{Dq})i_{1q} \\ \bar{i}_{11-} &= (K_{Ad} - K_{Bd} + K_{Cd} - K_{Dd})i_{1d} + \\ &\quad - j(K_{Aq} - K_{Bq} + K_{Cq} - K_{Dq})i_{1q} \end{aligned} \quad (34)$$

The equations in (34) show that, at steady state (i.e., constant  $i_{1d}$ ,  $i_{1q}$  and sharing coefficients), the current space vectors  $\bar{i}_{5-}$ ,  $\bar{i}_{7+}$  and  $\bar{i}_{11-}$  are constants. This allows tracking the reference currents with zero error at steady state.

### B. Control Scheme

The control system of the drive must adjust the d-q components  $i_{1d}$  and  $i_{1q}$  of the stator current SV  $\bar{i}_1$  according to the desired rotor flux and torque. The current SVs  $\bar{i}_5^S$ ,  $\bar{i}_7^S$  and  $\bar{i}_{11}^S$  are defined by (33). The setpoints for the current SVs  $\bar{i}_{5-}$ ,  $\bar{i}_{7+}$  and  $\bar{i}_{11-}$  depend on the value assumed by the main SV  $\bar{i}_1$  according to (34), hence they are indirectly affected by the speed/torque and rotor flux regulators. However, the machine equations (12) and (13) of subspaces 1, 5, 7 and 11 are independent of each others. This assumption is valid if the iron saturation and the machine asymmetries are negligible. Therefore, the control scheme of the machine can be implemented as shown in Fig. 5. PI regulator (a) controls the rotor flux by adjusting  $i_{1d}$ , while PI regulator (b) controls the speed by varying the torque-producing current  $i_{1q}$ ; PI regulators (d), (e) and (f) control the  $\bar{i}_{5-}$ ,  $\bar{i}_{7+}$  and  $\bar{i}_{11-}$ ; finally, the inverse transformation (11) is applied to the voltage vectors, and a suitable PWM strategy is used to control the four inverters (A,B,C,D).

It is worth noting that controllers (d), (e) and (f) consist of two PI regulators, respectively for the real and imaginary part of the current SVs. Therefore, the overall number of PI regulators for the current control is eight (four pairs).

If  $K_{Td} = K_{Tq} = K_T$ , (31) becomes:

$$\begin{aligned} \bar{i}_{5-} &= (K_A + jK_B - K_C + jK_D)\bar{i}_1^* \\ \bar{i}_{7+} &= (K_A - jK_B - K_C - jK_D)\bar{i}_1 \\ \bar{i}_{11-} &= (K_A - K_B + K_C - K_D)\bar{i}_1^* \end{aligned} \quad (35)$$

From (35), it is straightforward to note that, if all the sharing coefficients are equal to 1/4, the current SVs  $\bar{i}_{5-}$ ,  $\bar{i}_{7+}$  and  $\bar{i}_{11-}$  are set to zero. It is important to emphasize that these additional PI regulators are necessary even if the machine is controlled without imbalance among the inverter currents, because the additional current SVs must be maintained equal to zero. Consequently, the computational effort to control the machine is equal in a conventional control, a simplified standard current-sharing control (35) or the proposed d-q axis decoupled current-sharing control (34). Therefore, the control scheme can always be implemented as shown in Fig. 5.

## VI. EXPERIMENTAL RESULTS

The presented current sharing algorithms have been tested by means of a quadruple three-phase IM, which is a down-scaled prototype of a starter/generator for MEA applications. The test rig and the quadruple three-phase inverter are shown in Fig. 6. The IM is connected to the load through a gearbox, and the transferred torque is measured by a torque meter (Kistler 4503A50H00B1000). Fig. 6 (b) shows the inverter and the control platform. The inverter is based on four independent three-phase power modules, whereas the control platform is designed as a single unit (centralized control), which uses

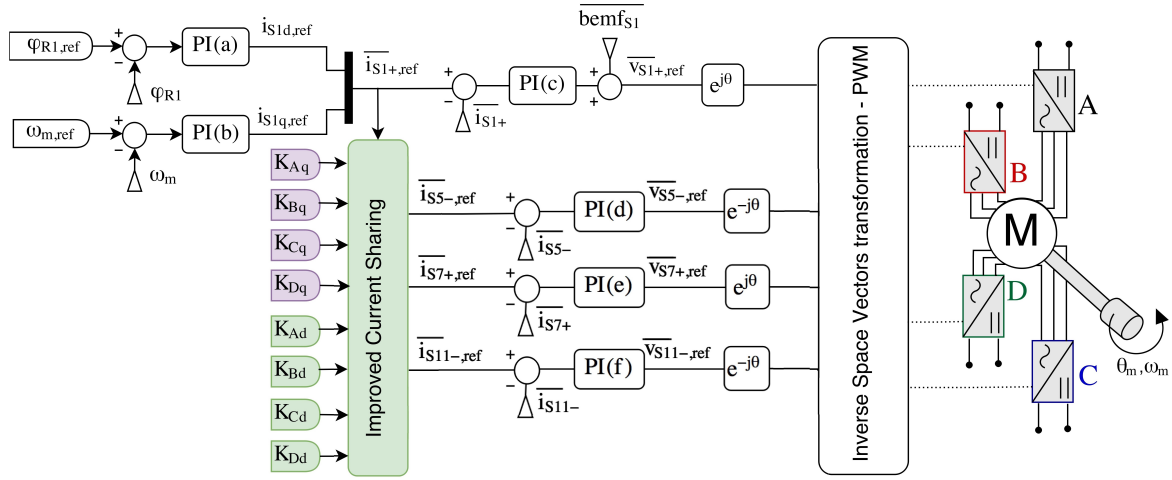


Fig. 5. Control architecture block diagram for a quadruple three-phase IM under standard or current sharing control.

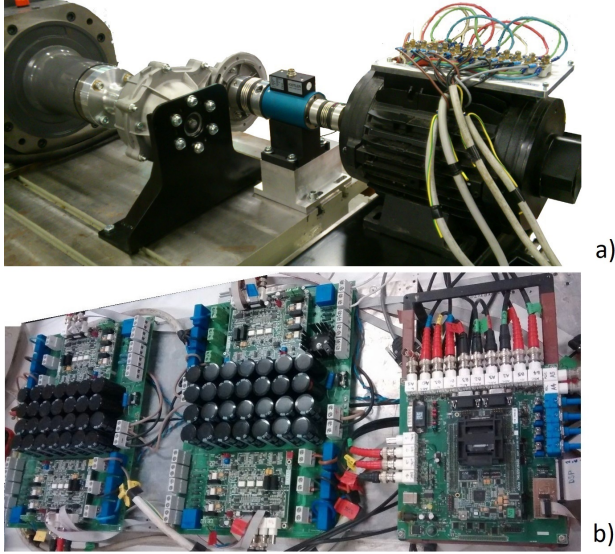


Fig. 6. Test bench. Scaled prototype of quadruple three-phase induction starter/generator and bidirectional drive (a); quadruple three-phase inverter and control board (b).

 TABLE I  
MAIN MACHINE PARAMETERS (50 Hz)

| Symbol                  | Quantity                      | Value               |
|-------------------------|-------------------------------|---------------------|
| $m$                     | number of phases              | 12 ( $4 \times 3$ ) |
| $p$                     | number of pole pairs          | 2                   |
| $N_b$                   | number of squirrel cage bars  | 40                  |
| $P_{rated}$             | rated power                   | 10 kW               |
| $ \bar{i}_{S,1,rated} $ | main current vector magnitude | 16 $A_{pk}$         |
| $i_{S,1,d,rated}$       | rated d-axis current          | 10 $A_{pk}$         |
| $I_{max}$               | maximum phase current         | 23 $A_{pk}$         |
| $ \bar{v}_{S,1,rated} $ | rated phase voltage           | 186 $V_{pk}$        |
| $R_S$                   | stator resistance             | 0.188 $\Omega$      |
| $R_R$                   | rotor resistance              | 0.156 $\Omega$      |
| $L_{S,1}, L_{R,1}$      | stator and rotor inductances  | 12.8 mH             |
| $M_1$                   | mutual inductance             | 12.0 mH             |

 TABLE II  
COMPARISON OF THE CURRENT SHARING CONTROLS FOR A  
QUADRUPLE THREE-PHASE SQUIRREL CAGE IM

| Sharing Algorithm   | Sharing Coefficients<br>[ $K_{dA}, K_{dB}, K_{dC}, K_{dD}$ ]<br>[ $K_{qA}, K_{qB}, K_{qC}, K_{qD}$ ] | Stator Copper<br>losses [W]<br>(experimental) |
|---|--|---|
| i) Normal operation   | [0.25, 0.25, 0.25, 0.25]<br>[0.25, 0.25, 0.25, 0.25]   | 119.85 (+0.00%)                               |
| ii) Unbalanced current sharing<br>(the current of inverter A is zero)   | [0.00, 0.33, 0.33, 0.33]<br>[0.00, 0.33, 0.33, 0.33]   | 158.25 (+32.04%)                              |
| iii) Unbalanced current sharing<br>(the reference torque of inverter A is zero)   | [0.25, 0.25, 0.25, 0.25]<br>[0.00, 0.33, 0.33, 0.33]   | 122.19 (+1.95%)                               |
| iv) Opposite current of inverter A  | [-0.25, 0.25, 0.5, 0.5]<br>[-0.25, 0.25, 0.5, 0.5]   | 297.54 (+148.16%)                             |
| v) Inverter A with opposite reference torque<br>of inverter B   | [0.25, 0.25, 0.25, 0.25]<br>[-0.25, 0.25, 0.5, 0.5]  | 131.49 (+9.71%)                               |
| vi) Unbalanced current sharing<br>(inverter A is controlled to produce only torque<br>whereas B, C and D are only used to control the rotor flux) | [0.00, 0.33, 0.33, 0.33]<br>[1.00, 0.00, 0.00, 0.00]   | 183.95 (+53.48%)                              |

a TMS320F28335 Digital Signal Processor (DSP). Table I presents the main machine parameters.

Fig. 7 shows the phase currents and the d-q components of the current SVs for each three-phase inverter in five different operating conditions of current sharing. The sub figures on the left show the transition of the d-q components of the current SVs of each three-phase inverter from balanced to unbalanced current-sharing operation, whereas those on the right illustrate the steady state waveforms of the phase currents.

The experimental tests were carried out at the rated magnetizing current ( $i_d = 10 A_{pk}$ ), and a speed of 600 rpm. The experimental results in Fig. 7 correspond to the following operating conditions:

- (i) standard operation (all inverters equally contribute to the control of the electromagnetic torque and the rotor flux):  $K_{Td} = K_{Tq} = 1/4$  for all the converters;
- (ii) unbalanced operation, where the output current of inverter A is set to zero (e.g., post-fault control algorithm);
- (iii) unbalanced operation, where the inverter A does not contribute to the electromagnetic torque, but all converters equally participate in the generation of the rotor flux:  $K_{Td} = 1/4$  for all the converters,  $K_{Aq} = 0$  and  $K_{Tq} = 0.333$  for the remaining inverters;
- (iv) the current is opposite in converters A and B, while the production of the electromagnetic torque and ro-

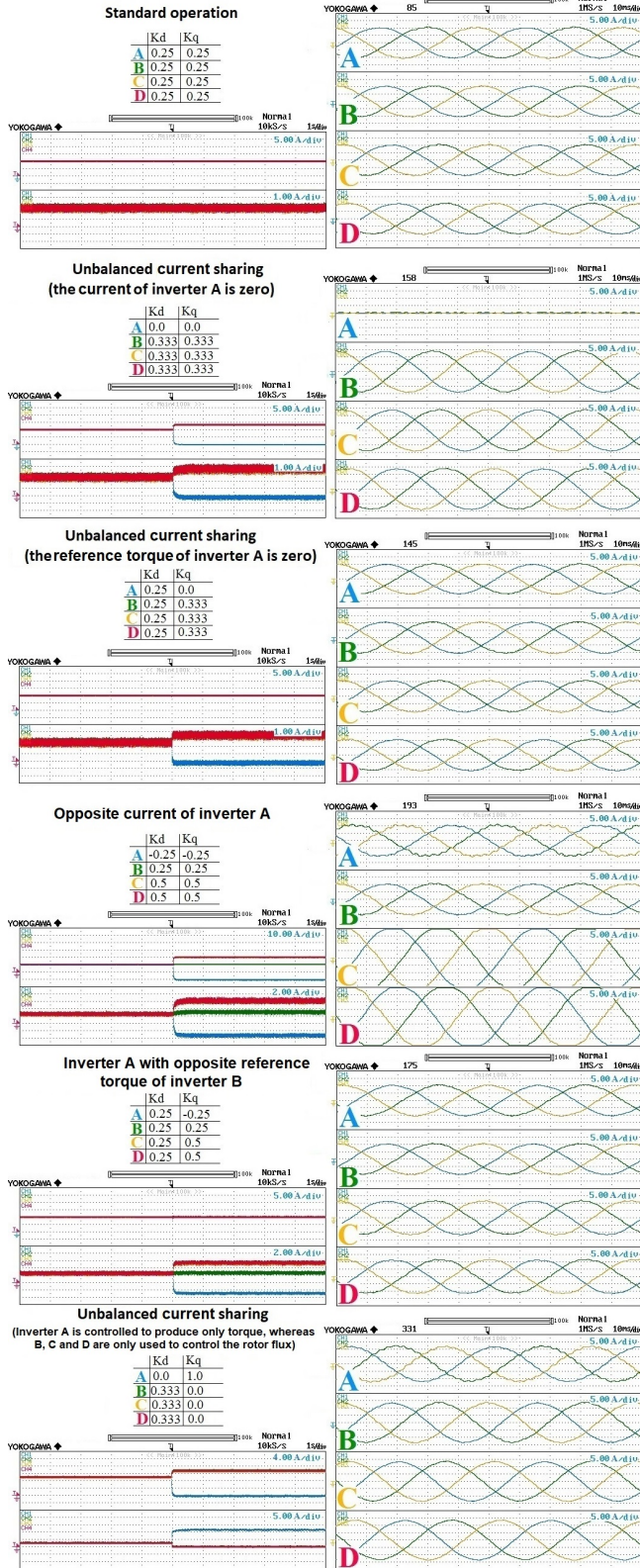


Fig. 7. Three-phase current SVs in the d-q plane and sharing coefficients (left), and phase currents of inverters A, B, C and D (right) in the six conditions of current sharing.

tor flux are equally split between inverter C and D:  $K_{Ad} = K_{Aq} = -K_{Bd} = -K_{Bq}$  and  $K_{Cd} = K_{Cq} =$

$$K_{Dd} = K_{Dq} = 0.5;$$

- (v) opposite setpoints for the torque-producing currents of inverters A and B, while the other converters equally participate to the generation of the motor torque:  $K_{Aq} = -K_{Bq}$  and  $K_{Cq} = K_{Dq} = 0.5$ . The inverters equally contribute to the control of the rotor flux:  $K_{Ad} = K_{Bd} = K_{Cd} = K_{Dd} = 0.25$ ;
- (vi) inverter A only contributes to the electromagnetic torque, while the generation of the rotor flux is equally shared among inverters B, C and D:  $K_{Ad} = 0$  and  $K_{Aq} = 1$ , while  $K_{Bd} = K_{Cd} = K_{Dd} = 0.333$  and  $K_{Bq} = K_{Cq} = K_{Dq} = 0$ .

In order to highlight its advantages, the developed decoupled current sharing algorithm is compared to the conventional one in two operating conditions. In the former, inverter A does not contribute to the electromagnetic torque (*ii* and *iii*). In the latter, the torque contribution of inverter A is opposite to the one of inverter B (*iv* and *v*).

Table II summarizes the stator Joule losses obtained at steady state for the experimental results shown in Fig. 7 in order to highlight how the current sharing affects the stator losses compared to the standard balanced operation, and how the d-q decoupling enhances the performance. The comparison of the current sharing algorithms shows that the proposed strategy significantly reduces the stator Joule losses in cases *iii-v* respectively compared with *ii-iv*. For example, in case *iv*, the conventional sharing algorithm requires a negative value of  $i_{1d}$  in inverter A, which generates a reduction in the rotor flux. Consequently, inverters C and D, which compensate the torque decrease produced by inverter A, have to further increase the d components of their phase currents to consider this reduction in the rotor flux. Conversely, as far as the proposed current sharing technique is concerned, the d component of the current vector is equal for all inverters, independently of how they contribute to the electromagnetic torque. For this particular case study, the reduction in the stator Joule losses with the proposed control algorithm is higher than 50%, as can be seen in Table II.

To carry out all the experimental tests of Fig. 7 under the same conditions of torque and flux, in particular when inverter A reverses the magnetizing current in case *iv*, it is necessary to limit significantly the values of the q component of the stator currents. Therefore, the current sharing algorithm has been validated at higher values of  $i_{1q}$ . In the experimental test of Fig. 8, all the four inverters equally contribute to the generation of the rotor flux, but not to the electromagnetic torque. In particular, the q component of inverter B, C and D is respectively twice, three times and four times that of inverter A. The operating condition with an equal repartition of the d components of the current vectors is the most relevant scenario. Fig. 8 shows the transient behaviour of the d-q components of the current SVs when the operating condition moves from balanced to unbalanced current sharing. The test was carried out at 1500 rpm, a magnetizing current of 10 A ( $i_{1d} = 10 A_{pk}$ ), and a q-axis current of 10 A ( $i_{1q} = 10 A_{pk}$ ). In Fig. 8, also the trajectories of the current space vector of the machine are shown. As expected, according to (32) and

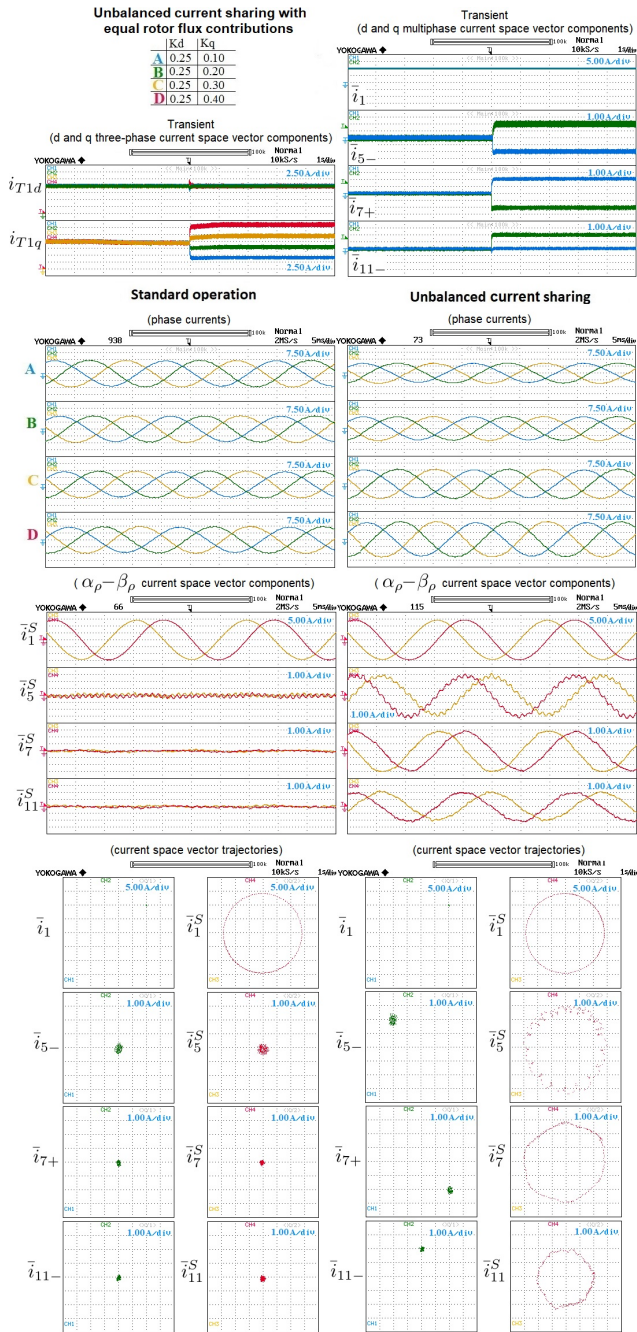


Fig. 8. Current sharing with equally distributed contributions of the inverters to the rotor flux production ( $i_d$ ):  $K_{Ad} = K_{Bd} = K_{Cd} = K_{Dd} = 0.25$ ;  $K_{Aq} = 0.1$ ,  $K_{Bd} = 0.2$ ,  $K_{Cd} = 0.3$ ,  $K_{Dd} = 0.4$ . At the top: three-phase and multiphase current space vector d-q axes components in the synchronous reference frames. At the bottom: comparison between standard and current sharing operation in terms of phase currents and multiphase currents space vectors.

(33), all the current SVs move on circular trajectories in the complex plane (subspace)  $\alpha_p - \beta_p$ . Therefore, as can be seen, the setpoints of the PI regulators used for the control of the auxiliary current SVs are constant, and the tracking error can be cancelled at steady state. The negative effects caused by the dead times and the nonlinearities of the inverters have been significantly reduced by means of additional compensation algorithms, based on an approach similar to that proposed in [26]. Some ripple still remains in the phase currents, mainly

associated with the control of the currents mapped in the 5<sup>th</sup> subspace.

## VII. CONCLUSION

This paper compares different current sharing algorithms for the control of multi three-phase IMs. In particular, the proposed method is based on the d-q decomposition of the reference current vector of each three-phase inverter, in order to independently adjust the contribution to the generation of the electromagnetic torque and rotor flux. The decoupled current sharing algorithm is presented in a comprehensive manner for an arbitrary number of three-phase windings, and the setpoints for the minimum stator Joule losses are deduced directly from the machine analytical model.

The control architecture and the methodology for the definition of the reference frames used for the implementation of the PI regulators are explained. The possibility to implement the algorithm without requiring additional PI regulators in comparison with the standard control scheme makes this method a valid solution for the current sharing control of multi three-phase IMs.

This work aims to give a contribution to the state of the art in the control of multi three-phase electrical drives where independent current setpoints are desired for the three-phase subsystems.

## REFERENCES

- [1] E. Levi, R. Bojoi, F. Profumo, H. A. Toliyat, and S. Williamson, "Multiphase induction motor drives - a technology status review," *IET Electric Power Applications*, vol. 1, no. 4, pp. 489–516, Jul. 2007.
- [2] V. Yaramasu, B. Wu, P. C. Sen, S. Kouro, and M. Narimani, "High-power wind energy conversion systems: State-of-the-art and emerging technologies," *Proc. IEEE*, vol. 103, no. 5, pp. 740–788, May. 2015.
- [3] J. Dai, S. W. Nam, M. Pande, and G. Esmaili, "Medium-voltage current-source converter drives for marine propulsion system using a dual-winding synchronous machine," *IEEE Transactions on Industry Applications*, vol. 50, no. 6, pp. 3971–3976, Nov. 2014.
- [4] A. Tesserolo, G. Zocco, and C. Tonello, "Design and testing of a 45-mw 100-hz quadruple-star synchronous motor for a liquefied natural gas turbo-compressor drive," *IEEE Transactions on Industry Applications*, vol. 47, no. 3, pp. 1210–1219, May. 2011.
- [5] R. Bojoi, A. Cavagnino, A. Tenconi, and S. Vaschetto, "Control of shaft-line-embedded multiphase starter/generator for aero-engine," *IEEE Transactions on Industrial Electronics*, vol. 63, no. 1, pp. 641–652, 2016.
- [6] A. Cavagnino, Z. Li, A. Tenconi, and S. Vaschetto, "Integrated generator for more electric engine: Design and testing of a scaled-size prototype," *IEEE Transactions on Industry Applications*, vol. 49, no. 5, pp. 2034–2043, Sep. 2013.
- [7] E. Jung, H. Yoo, S. Sul, H. Choi, and Y. Choi, "A nine-phase permanent-magnet motor drive system for an ultrahigh-speed elevator," *IEEE Transactions on Industry Applications*, vol. 48, no. 3, pp. 987–995, 2012.
- [8] A. Cavagnino, A. Tenconi, and S. Vaschetto, "Experimental characterization of a belt-driven multiphase induction machine for 48-v automotive applications: Losses and temperatures assessments," *IEEE Transactions on Industry Applications*, vol. 52, no. 2, pp. 1321–1330, Mar. 2016.
- [9] M. R. Arahal, C. Martin, F. Barrero, I. Gonzalez-Prieto, and M. J. Duran, "Model-based control for power converters with variable sampling time: A case example using five-phase induction motor drives," *IEEE Transactions on Industrial Electronics*, Early Access, 2018.
- [10] L. Zarri, M. Mengoni, A. Tani, G. Serra, and D. Casadei, "Minimization of the power losses in igbt multiphase inverters with carrier-based pulsewidth modulation," *IEEE Transactions on Industrial Electronics*, vol. 57, no. 11, pp. 3695–3706, Nov. 2010.
- [11] J. K. Pandit, M. V. Aware, R. V. Nemade, and E. Levi, "Direct torque control scheme for a six-phase induction motor with reduced torque ripple," *IEEE Transactions on Power Electronics*, vol. 32, DOI 10.1109/TPEL.2016.2624149, no. 9, pp. 7118–7129, Sep. 2017.

- [12] G. Sala, G. Valente, A. Formentini, L. Papini, D. Gerada, P. Zanchetta, A. Tani, and C. Gerada, "Space vectors and pseudoinverse matrix methods for the radial force control in bearingless multisection permanent magnet machines," *IEEE Transactions on Industrial Electronics*, vol. 65, no. 9, pp. 6912–6922, Sep. 2018.
- [13] K. Wang, "Effects of harmonics into magnet shape and current of dual three-phase permanent magnet machine on output torque capability," *IEEE Transactions on Industrial Electronics*, vol. 65, no. 11, pp. 8758–8767, 2018.
- [14] F. Luise, S. Pieri, M. Mezzarobba, and A. Tassarolo, "Regenerative testing of a concentrated winding permanent magnet synchronous machine for offshore wind generation part i: Test concept and analysis," *IEEE Transactions on Industry Applications*, vol. 48, no. 6, pp. 1779–1790, 2012.
- [15] F. Luise, S. Pieri, M. Mezzarobba, and A. Tassarolo, "Regenerative testing of a concentrated winding permanent magnet synchronous machine for offshore wind generation part ii: Test implementation and results," *IEEE Transactions on Industry Applications*, vol. 48, no. 6, pp. 1791–1796, 2012.
- [16] A. Galassini, A. Costabeber, M. Degano, C. Gerada, A. Tassarolo, and R. Menis, "Enhanced power sharing transient with droop controllers for multithree-phase synchronous electrical machines," *IEEE Transactions on Industrial Electronics*, vol. 66, no. 7, pp. 5600–5610, 2019.
- [17] M. Zabaleta, E. Levi, and M. Jones, "A novel synthetic loading method for multiple three-phase winding electric machines," *IEEE Transactions on Energy Conversion*, vol. 34, no. 1, pp. 70–78, 2019.
- [18] S. Rubino, R. Bojoi, S. A. Odhano, and P. Zanchetta, "Model predictive direct flux vector control of multi-three-phase induction motor drives," *IEEE Transactions on Industry Applications*, vol. 54, no. 5, pp. 4394–4404, 2018.
- [19] H. S. Che, E. Levi, M. Jones, M. J. Duran, W. Hew, and N. A. Rahim, "Operation of a six-phase induction machine using series-connected machine-side converters," *IEEE Transactions on Industrial Electronics*, vol. 61, no. 1, pp. 164–176, 2014.
- [20] I. Zoric, M. Jones, and E. Levi, "Arbitrary power sharing among three-phase winding sets of multiphase machines," *IEEE Transactions on Industrial Electronics*, vol. 65, no. 2, pp. 1128–1139, Feb. 2018.
- [21] A. Tani, G. Serra, M. Mengoni, L. Zarri, G. Rini, and D. Casadei, "Dynamic stator current sharing in quadruple three-phase induction motor drives," in *IECON 2013 - 39th Annual Conference of the IEEE Industrial Electronics Society*, pp. 5173–5178, Vienna, Austria, 10–13 Nov 2013.
- [22] M. Mengoni, G. Sala, L. Zarri, A. Tani, G. Serra, Y. Gritli, and M. Duran, "Control of a fault-tolerant quadruple three-phase induction machine for more electric aircrafts," in *IECON 2016 - 42nd Annual Conference of the IEEE Industrial Electronics Society*, pp. 5747–5753, 2016.
- [23] M. J. Duran, I. Gonzalez-Prieto, A. Gonzalez-Prieto, and F. Barrero, "Multiphase energy conversion systems connected to microgrids with unequal power-sharing capability," *IEEE Transactions on Energy Conversion*, vol. 32, no. 4, pp. 1386–1395, 2017.
- [24] G. Sala, P. Girardini, M. Mengoni, L. Zarri, A. Tani, and G. Serra, "Comparison of fault tolerant control techniques for quadruple three-phase induction machines under open-circuit fault," in *2017 IEEE 11th International Symposium on Diagnostics for Electrical Machines, Power Electronics and Drives (SDEMPED)*, pp. 213–219, 2017.
- [25] M. J. Duran, I. Gonzalez-Prieto, N. Rios-Garcia, and F. Barrero, "A simple, fast, and robust open-phase fault detection technique for six-phase induction motor drives," *IEEE Transactions on Power Electronics*, vol. 33, no. 1, pp. 547–557, 2018.
- [26] H. S. Che, E. Levi, M. Jones, W. Hew, and N. A. Rahim, "Current control methods for an asymmetrical six-phase induction motor drive," *IEEE Transactions on Power Electronics*, vol. 29, no. 1, pp. 407–417, 2014.



**G. Sala** received the B. Sc. in Power Engineering in 2012, the M. Sc. degree with honors in Electrical Engineering in 2014, and the Ph. D. in Electrical Machines and Drives in 2018 from the University of Bologna, Bologna, Italy. He was a researcher with the Department of Electrical and Electronic Engineering (PEMC group), at The University of Nottingham, until 2019. He joined the Department of Electrical, Electronic and Information Engineering "G. Marconi", University of Bologna, where he has been a research fellow since 2019. His research interests include design, modelling and control of multiphase machines and drives.



**M. Mengoni** (M'13) received the M.S. (with honors) and Ph.D. degrees in electrical engineering from the University of Bologna, Bologna, Italy, in 2006 and 2010, respectively. He is currently a Senior Assistant Professor with the Department of Electrical, Electronic and Information Engineering "G. Marconi", University of Bologna. His research interests include design, analysis, and control of three phase electric machines, multiphase drives, and ac/ac matrix converters.



**G. Rizzoli** received the M.Sc and Ph.D. degree in Electrical Engineering, with honors, respectively in 2012 and 2016, from the University of Bologna, Bologna, Italy. In 2014 he was the recipient of the Best Paper Award at the IEEE International Electric Vehicle Conference 2014 (IEVC 2014). In 2015 he was a visiting student at Virginiatech (CPES), Blacksburg, Virginia, United States of America. He is currently a research fellow at the Department of Electrical, Electronic and Information Engineering "G. Marconi" of the University of Bologna. His research interests include the design of electrical machines, the development and control of high-efficient power converters for automotive and renewable energy applications.



**L. Zarri** (M'05-SM'12) received the M. Sc. and Ph.D. degree in Electrical Engineering from the University of Bologna, Bologna, Italy, in 1998 and 2007, respectively. Currently, he is an Associate Professor with the Department of Electrical, Electronic and Information Engineering "G. Marconi", University of Bologna. He has authored or coauthored more than 150 scientific papers. His research activity concerns the control of power converters and electric drives. He is a senior member of the IEEE Industry Applications, IEEE Power Electronics and IEEE Industrial Electronics Societies.



**A. Tani** received the M. Sc. degree in Electrical Engineering, with honors, from the University of Bologna, Bologna, Italy, in 1988. Currently he is a Full Professor of power electronics, electrical machines and drives with the Department of Electrical, Electronic and Information Engineering "G. Marconi", University of Bologna. He has authored more than 180 papers published in technical journals and conference proceedings. His current activities include multiphase and three phase electric drives, diagnostic techniques for electric machines, and active filters.